

# L4acados: Learning-based models for acados, applied to Gaussian process-based predictive control

Amon Lahr<sup>1,\*</sup>, Joshua Näf<sup>1</sup>, Kim P. Wabersich<sup>2</sup>, Jonathan Frey<sup>3</sup>, Pascal Siehl<sup>2</sup>,  
Andrea Carron<sup>1</sup>, Moritz Diehl<sup>3</sup>, Melanie N. Zeilinger<sup>1</sup>

**Abstract**—Incorporating learning-based models, such as artificial neural networks or Gaussian processes, into model predictive control (MPC) strategies can significantly improve control performance and online adaptation capabilities for real-world applications. Still, enabling state-of-the-art implementations of learning-based models for MPC is complicated by the challenge of interfacing machine learning frameworks with real-time optimal control software. This work aims at filling this gap by incorporating external sensitivities in sequential quadratic programming solvers for nonlinear optimal control. To this end, we provide **L4acados**, a general framework for incorporating Python-based residual models in the real-time optimal control software **acados**. By computing external sensitivities via a user-defined Python module, **L4acados** enables the implementation of MPC controllers with learning-based residual models in **acados**, while supporting parallelization of sensitivity computations when preparing the quadratic subproblems. We demonstrate significant speed-ups and superior scaling properties of **L4acados** compared to available software using a neural-network-based control example. Last, we provide an efficient and modular real-time implementation of Gaussian process-based MPC using **L4acados**, which is applied to two hardware examples: autonomous miniature racing, as well as motion control of a full-scale autonomous vehicle for an ISO lane change maneuver.

**Code:** <https://github.com/IntelligentControlSystems/l4acados>

**Index Terms**—Predictive control for nonlinear systems, control software, machine learning.

## I. INTRODUCTION

**A**UGMENTING physics-based prediction models with learning-based components, such as neural networks or Gaussian processes, has shown to be a data-efficient way to improve their prediction accuracy at reduced modeling effort. Leveraging the improved prediction capabilities in model predictive control (MPC) architectures [1], the gray-box modeling approach has shown to be highly effective for challenging applications such as autonomous driving [2]–[4], drone control [5]–[9] outdoor mobile robots [10], [11] and other robotic applications [12].

\*Corresponding author.

<sup>1</sup>ETH Zurich, Zurich, Switzerland. E-mail correspondence to {amlahr, naefjo, carrona, mzeilinger}@ethz.ch.

<sup>2</sup>Robert Bosch GmbH, Corporate Research, Stuttgart, Germany. E-mail: {kimpeter.wabersich, pascal.siehl}@de.bosch.com.

<sup>3</sup>Department of Microsystems Engineering (IMTEK) and Department of Mathematics, University of Freiburg, Freiburg, Germany. E-mail: {jonathan.frey, moritz.diehl}@imtek.uni-freiburg.de

This work was supported by the European Union’s Horizon 2020 research and innovation programme, Marie Skłodowska-Curie grant agreement No. 953348, ELO-X, and by DFG via 424107692 and 504452366 (SPP 2364).

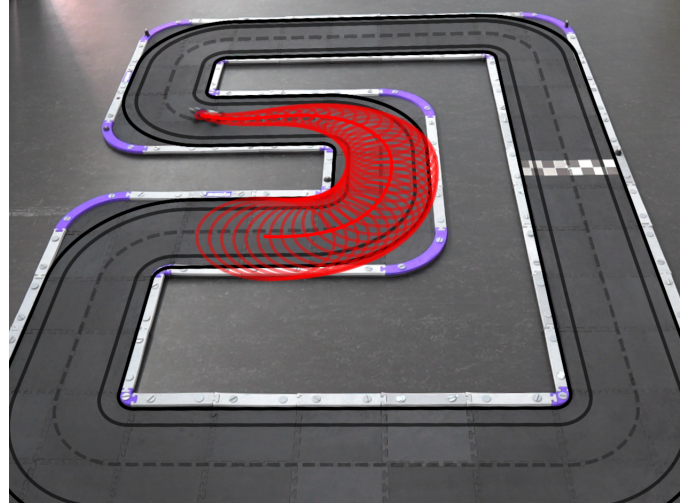


Fig. 1. Real-time GP-MPC implementation with **L4acados** applied to autonomous miniature racing; uncertainty-aware predictions of the open-loop state trajectory are shown in red. **L4acados** enables efficient and parallelized external sensitivity computations of the Gaussian process model. The modular and open-source GP-MPC implementation supports arbitrary GPyTorch GP models, fast covariance propagation, and various data processing strategies for online adaptation of the GP model.

Yet, while significant advancements have been made in computationally efficient inference and automatic differentiation for learning-based models [13]–[15], enabling these for MPC applications remains challenging due to the difficulty of interfacing machine learning frameworks, such as JAX [13], PyTorch [14], TensorFlow [15], with embedded optimal control software, such as CasADi [16] and acados [17]. In particular for fast-sampled model predictive control applications, the combination of CasADi and acados has become a popular choice, with CasADi providing a sparsity-exploiting automatic differentiation engine and acados implementing fast solvers for real-time embedded optimal control.

In this paper, we bridge this gap by incorporating external sensitivity information through modification of model parameters at each iteration of the MPC solver. Specifically, we provide **L4acados**, which enables Python-based sensitivities for real-time optimal control with acados. The efficiency of the implementation is demonstrated for learning-based MPC with neural network and Gaussian process models, applied in a benchmark against available software in simulation and on two hardware platforms for autonomous driving, respectively.

### Related work

Existing real-time learning-based MPC applications commonly resort to custom (re-)implementations of the chosen learning-based model architecture in CasADi [7], [9], [18]–[21], lagging behind the state-of-the-art in terms of available methods, computational efficiency, parallelization capabilities and ease of use. An alternative approach is to locally approximate the learning-based model as a constant parameter [5], [8] or using a second-order approximation [22], reducing the number of model (Jacobian) evaluations at the expense of an approximate MPC solution.

Available software frameworks for learning-based optimal control generally employ similar strategies to incorporate sensitivities of learning-based models: For MPC with neural-network models, do-mpc [23] imports models adhering to the ONNX [24] standard as CasADi models. Similarly, HILO-MPC [25] supports artificial neural networks and vanilla GP regression by re-implementing them within CasADi. For Gaussian process-based MPC (GP-MPC), LbMATMPC [26] re-implements the GP posterior mean and its Jacobian in CasADi as a vector product with precomputed weights. In the safe-control-gym [18] GP-MPC implementation, GP inference is partly manually formulated with CasADi symbolics and partly directly evaluated in GPyTorch. A more general approach is followed by L4CasADi [27], enabling the integration of PyTorch models by compiling them into the CasADi computational graph. Yet, beyond the restriction to traceable PyTorch models, L4CasADi's batch processing capabilities are not compatible with the available options for parallelized sensitivity computation in acados, complicating the efficient integration of both tools.

In particular for Gaussian process-based MPC [3], aside from the coupling between efficient inference algorithms and optimal control software, an additional difficulty is posed by the complexity of the uncertainty-aware optimal-control problem formulation. For computational tractability, state covariances are thus largely not considered inside the optimization problem [5], [10], [26], [28], or heuristically fixed based on the state-input trajectory obtained at the previous sampling time of the model predictive controller [2], [3], [12], [29]. This problem has been alleviated by leveraging the zero-order robust optimization (zoRO) algorithm, which obtains a sub-optimal, yet feasible, point of the OCP at drastically reduced computation cost. The zoRO algorithm, initially proposed in the stochastic [30] and later in the robust MPC setting [31], has seen successful applications in obstacle avoidance problems using nonlinear robust MPC [32], as well as for friction-adaptive autonomous driving [33]. For GP-MPC, the zoRO algorithm has been analyzed by [34]; similar optimization strategies have also been employed by [11], using a log-barrier constraint relaxation for control of an outdoor robot, and by [35], employing a linear-parameter-varying reformulation of the GP-MPC problem. Still, existing efficient and open-source implementations are tailored to their specific use-case [18], [34], limiting their widespread application.

### Contribution

The contribution of this paper is two-fold. First, we propose a method to integrate external sensitivity information into sequential quadratic programming (SQP) solvers for nonlinear model predictive control using learning-based residual models. To this end, we provide L4acadoss – an efficient implementation thereof in the real-time optimal control software acados. The framework supports general Python-callable residual models, Real-Time Iterations (RTI) [36], as well as parallelization of the model and Jacobian evaluation during the RTI preparation phase. The computational efficiency of the proposed approach is demonstrated in a benchmark against available software for learning-based MPC using a neural-network-based residual model.

Second, utilizing L4acadoss, we provide an efficient, modular implementation of Gaussian process-based MPC for real-time applications. Therefore, we extend the recently developed, efficient implementation of the zoRO algorithm [37] to the zero-order GP-MPC (zoGPMPC) [34] setting. The fast GP-MPC implementation supports arbitrary GPyTorch [38] (approximate) GP models, as well as data processing strategies for online-learning applications, which are demonstrated in simulation and hardware on the automotive miniature racing platform CRS [39]. Last, L4acadoss is used to implement a GP-MPC motion controller for an ISO lane change maneuver with a full-scale autonomous vehicle.

## II. PROBLEM SETUP

We are concerned with real-time optimal control of nonlinear dynamical systems of the form

$$x(t+1) = f(x(t), u(t)) + B_d g^{\text{r}}(x(t), u(t)) + w(t), \quad (1)$$

where  $x(t) \in \mathbb{R}^{n_x}$  denotes the state of the system,  $u(t) \in \mathbb{R}^{n_u}$ , the applied control input, and  $w(t) \in \mathbb{R}^{n_x}$ , process noise. The ground-truth dynamics are split into a known, nominal part of the system dynamics,  $f : \mathbb{R}^{n_x \times n_u} \rightarrow \mathbb{R}^{n_x}$ , and an unknown residual,  $g^{\text{r}} : \mathbb{R}^{n_x \times n_u} \rightarrow \mathbb{R}^{n_x}$ . The residual affects certain components of the full state through the matrix  $B_d \in \mathbb{R}^{n_x \times n_g}$ , which is assumed to have full column rank. While the nominal model is commonly obtained by numerically integrating a continuous-time model based on first principles, an estimate  $g : \mathbb{R}^{n_x \times n_u} \rightarrow \mathbb{R}^{n_g}$  of the unknown residual can be obtained directly in discrete-time, for example, by training a learning-based regression model using subsequent state measurements of the true system, i.e.,

$$y(t) \doteq B_d^\dagger (x(t+1) - f(x(t), u(t))) \quad (2)$$

$$= g^{\text{r}}(x(t), u(t)) + v(t). \quad (3)$$

Here, the measurements  $y(t)$  are obtained by projecting the full state onto the subspace of the residual model using the Moore-Penrose pseudo-inverse  $(\cdot)^\dagger$  of  $B_d$ ; the corresponding measurement noise is given by  $v(t) = B_d^\dagger w(t)$ .

Using the learning-based model, a generic MPC controller computes the control input for system (1) at each sampling

time as  $u(t) = u_0^*(x(t))$ , where  $u_0^*(x(t))$  is the first component of the optimal input sequence solving the following OCP:

$$\min_{\substack{u_0, \dots, u_{N-1} \\ x_0, \dots, x_N}} \sum_{k=0}^{N-1} l(x_k, u_k) + M(x_N) \quad (4a)$$

$$\text{s.t. } x_0 = x(t), \quad (4b)$$

$$x_{k+1} = f(x_k, u_k) + B_{dg}(x_k, u_k), \quad (4c)$$

$$0 \geq h(x_k, u_k), \quad (4d)$$

$$0 \geq h_N(x_N). \quad (4e)$$

Hereby, the cost (4a) to be minimized consists of stage cost terms  $l: \mathbb{R}^{n_x \times n_u} \rightarrow \mathbb{R}$  and a terminal cost  $M: \mathbb{R}^{n_x} \rightarrow \mathbb{R}$ ; it is subject to the initial condition (4b), the learning-based dynamics (4c) along the prediction horizon  $k = 0, \dots, N-1$ , as well as stage-wise and terminal constraints (4d) and (4e), respectively.

### III. L4ACADOS: LEARNING-BASED MODELS FOR ACADOS

Software frameworks for embedded nonlinear model predictive control commonly query sensitivities of the cost, dynamics and constraint functions in (4) based on symbolic expressions for the dynamics model and constraints or a direct user interface to provide the function evaluations and sensitivities, see, e.g., [17], [40]–[44]. In the following, we present how, alternatively, external dynamics sensitivities may be included in the SQP algorithm (Section III-A) by parametrizing the nonlinear program. Afterwards, we introduce `L4acados`, an efficient implementation for external sensitivities in the real-time optimal control software `acados` (Section III-B), and demonstrate its performance benefits for learning-based MPC using neural networks compared to interfacing external sensitivities with `L4CasADi` (Section III-C).

#### A. External sensitivities for SQP solvers

Nonlinear programs of the form (4), which include (13) and (17), can be solved using sequential quadratic programming [45]. In each SQP iteration, the quadratic subproblem

$$\min_{\substack{\Delta u_0, \dots, \Delta u_{N-1} \\ \Delta x_0, \dots, \Delta x_N}} \sum_{k=0}^{N-1} \begin{bmatrix} \Delta x_k \\ \Delta u_k \\ 1 \end{bmatrix}^\top \begin{bmatrix} Q_k & S_k & q_k \\ & R_k & r_k \\ \star & & 1 \end{bmatrix} \begin{bmatrix} \Delta x_k \\ \Delta u_k \\ 1 \end{bmatrix} \quad (5a)$$

$$\text{s.t. } \Delta x_0 = 0 \quad (5b)$$

$$\begin{aligned} \Delta x_{k+1} = & f(\hat{x}_k, \hat{u}_k) + B_{dg}(\hat{x}_k, \hat{u}_k) - \hat{x}_{k+1} \\ & + \hat{A}_k \Delta x_k + \hat{B}_k \Delta u_k, \end{aligned} \quad (5c)$$

$$0 \geq h(\hat{x}_k, \hat{u}_k) + \hat{H}_k^x \Delta x_k + \hat{H}_k^u \Delta u_k, \quad (5d)$$

$$0 \geq h(\hat{x}_N) + \hat{H}_N^x \Delta x_N, \quad (5e)$$

is solved for increments  $\hat{x}_k \leftarrow \hat{x}_k + \Delta x_k$ ,  $\hat{u}_k \leftarrow \hat{u}_k + \Delta u_k$  to the current iterate. Thereby,  $Q_k, R_k, S_k$  define the employed approximation of the Lagrangian's Hessian and  $q_k, r_k$ , the

cost Jacobian at stage  $k$ . The original nonlinear equality and inequality constraints (4b)–(4e) are linearized, with Jacobians

$$\hat{A}_k = \left. \frac{\partial(f + B_{dg})}{\partial x} \right|_{\substack{x=\hat{\mu}_k^x \\ u=\hat{u}_k}}, \quad \hat{B}_k = \left. \frac{\partial(f + B_{dg})}{\partial u} \right|_{\substack{x=\hat{\mu}_k^x \\ u=\hat{u}_k}}, \quad (6)$$

$$\hat{H}_k^{\{x,u\}} = \left. \frac{\partial h}{\partial \{x, u\}} \right|_{\substack{x=\hat{\mu}_k^x \\ u=\hat{u}_k}}, \quad \hat{H}_N = \left. \frac{\partial h_N}{\partial x} \right|_{x=\hat{\mu}_k^x}. \quad (7)$$

Utilizing the fact that each SQP iteration does not require access to the full dynamics and constraint sensitivities, but merely their evaluations *at the current iterate*, the same SQP iterates can be obtained by reformulating the nonlinear program (4) based on the linearized dynamics (5c): Instead of the original OCP with nonlinear dynamics, consider the following OCP with affine dynamics, i.e.,

$$\min_{\substack{u_0, \dots, u_{N-1} \\ x_0, \dots, x_N}} \sum_{k=0}^{N-1} l(x_k, u_k) + M(x_N) \quad (8a)$$

$$\text{s.t. } x_0 = \bar{x}_0 \quad (8b)$$

$$x_{k+1} = \hat{A}_k x_k + \hat{B}_k u_k + \hat{c}_k, \quad (8c)$$

$$0 \geq h(x_k, u_k), \quad (8d)$$

$$0 \geq h_N(x_N), \quad (8e)$$

where  $\hat{A}_k, \hat{B}_k$  and  $\hat{c}_k$  are treated as model parameters. Setting

$$\hat{c}_k \doteq f(\hat{x}_k, \hat{u}_k) + B_{dg}(\hat{x}_k, \hat{u}_k) - \hat{A}_k \hat{x}_k - \hat{B}_k \hat{u}_k \quad (9)$$

and  $\hat{A}_k, \hat{B}_k$  at each SQP iteration according to (6) recovers the original dynamics linearization (5c) exactly. Hence, solving (4) and (8) using SQP under the same Hessian approximation in Eq. (5a) leads to the exact same iterates. This is the case for Hessian approximations that do not depend on second-order information of the dynamics, such as the generalized Gauss-Newton approximation. In a similar fashion, it is also possible to incorporate external sensitivity information into the cost and constraints of the OCP.

Next, we provide an efficient implementation of external sensitivities for `acados` [17], a popular software package providing fast OCP solvers and numerical integrators for embedded optimization.

#### B. L4acados: Learning-based models for acados

Within `acados`, the sensitivities in Eq. (6) are automatically computed based on the symbolic `CasADi` [16] expressions for the dynamics model. As `CasADi` is in general not compatible with learning-based residual models based on other automatic differentiation tools – with the exception of trace-able `PyTorch` models that can be interfaced through `L4CasADi` [27] – this complicates their use for real-time optimal control with `acados`. To tackle this challenge, we present `L4acados`, a general software framework to incorporate learning-based models from state-of-the-art machine learning packages such as `PyTorch` [14], `TensorFlow` [15] and `JAX` [13], into `acados`.



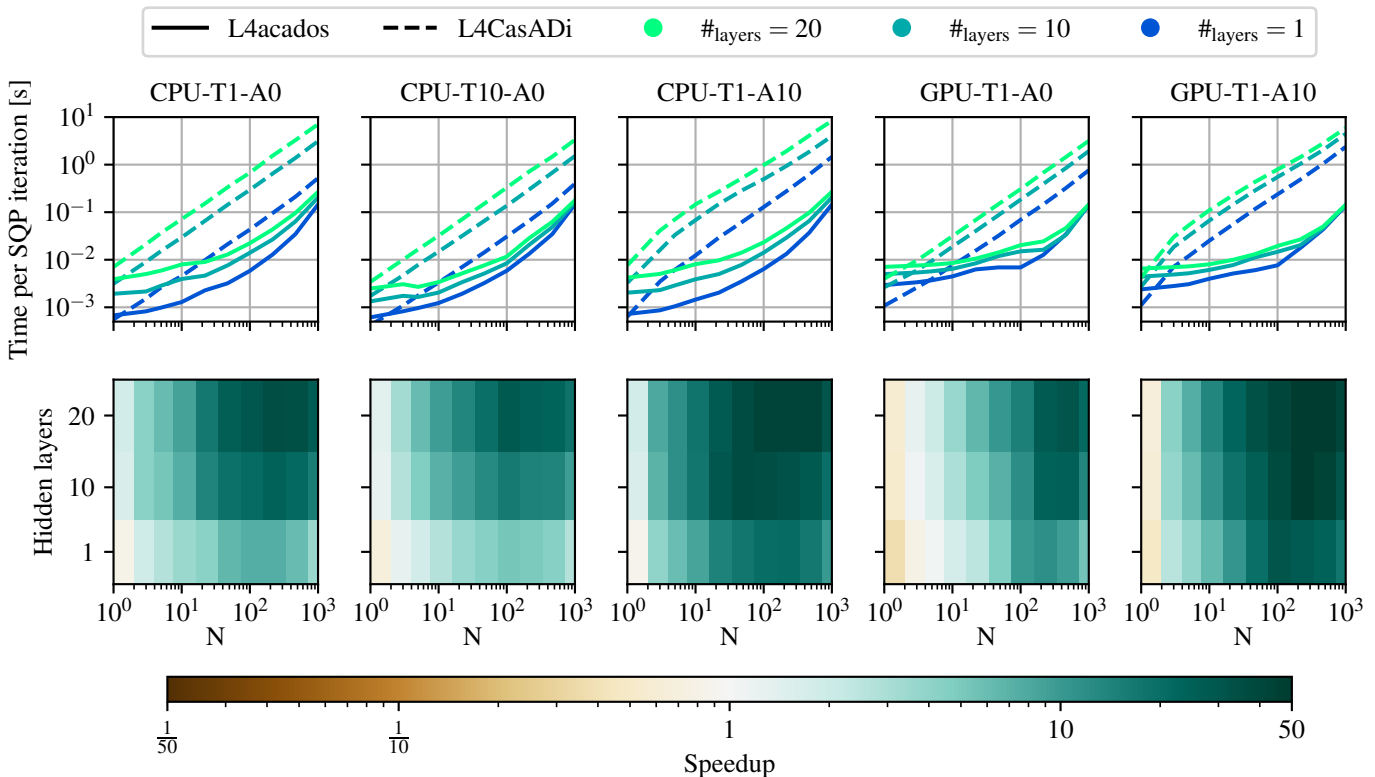


Fig. 3. Comparison of solve times for a neural-network residual model (Section III-C). Already for small horizon lengths and moderate learning-based-model complexities, L4acados shows drastic speedups compared to using acados with L4CasADi.

of the PyTorch multi-layer perceptron), and parallelization configurations “DEV-TX-AY”. Here,  $DEV \in \{\text{CPU}, \text{GPU}\}$  indicates whether the NN is evaluated on the CPU or GPU (with CUDA), respectively;  $X$ , the number of respective CPU cores in case of CPU parallelization; and  $Y$ , the number of CPU cores used for parallelizing the sensitivity evaluation in acados with OpenMP, where  $Y = 0$  denotes that acados is compiled without OpenMP parallelization.

Across all parallelization configurations considered, L4acados already achieves noticeable speedups for typically-short prediction horizons  $N \geq 10$ , which become more pronounced as the model complexity is increased. Parallelization of the NN evaluations on the CPU (“CPU-T10-”) or GPU (“GPU-T1-”) thereby leads to slight speedups for  $\#_{\text{layers}} = 20$  layers for both approaches; for fewer layers, to slightly larger computation times. Most prominent is the different scaling for varying lengths of the prediction horizon: For L4CasADi, the linear scaling of the computation time for all “-A0” scenarios is due to the sequential sensitivity computation in acados. For all “-A10” scenarios, it can be seen that using acados’ built-in OpenMP parallelization of sensitivity computations in conjunction with L4CasADi affects its scaling properties; however, it does not lead to computational benefits<sup>2</sup>. In contrast, by computing sensitivities in parallel outside acados, L4acados shows an improved

scaling throughout all scenarios, approaching the linear scaling as the ratio between available cores and horizon length decreases. Parallelization of the sensitivity evaluations for the “CPU-T1-A10” scenario has a negligible effect on the L4acados timings, as the sensitivity computations within acados, corresponding to the linearized dynamics, are trivial.

#### IV. GAUSSIAN PROCESS-BASED MPC USING L4ACADOS

In this section, L4acados is used for an efficient implementation of GP-MPC (Sections IV-A to IV-C), and applied both in simulation and hardware for real-time control on two autonomous driving platforms (see Fig. 4): miniature racing using CRS [39] (Section IV-D) and motion control of a full-scale vehicle for an ISO lane change maneuver (Section IV-E).

We begin by introducing the GP-MPC optimal control problem formulation (Section IV-A) as well as its efficient solution using a zero-order optimization algorithm (Section IV-B).

##### A. Gaussian process-based MPC formulation

As a special case of learning-based MPC, Gaussian process-based MPC estimates the residual dynamics  $g^{\text{tr}}$ , as well as the associated prediction uncertainty, using a Gaussian process

$$g^{\text{tr}} \sim \mathcal{GP}(g, \Sigma^g), \quad (12)$$

with posterior mean  $g : \mathbb{R}^{n_x \times n_u} \rightarrow \mathbb{R}^{n_g}$  and posterior covariance  $\Sigma^g : \mathbb{R}^{n_x \times n_u} \rightarrow \mathbb{R}^{n_g \times n_g}$ . In this setting, the process

<sup>2</sup>Using both L4CasADi and acados with OpenMP parallelization, i.e., “CPU-T10-A10”, led to considerably slower computation times as well as leaked memory at every solver call, and is thus not shown here.

noise is assumed to be Gaussian i.i.d., i.e.,  $w(t) \sim \mathcal{N}(0, \Sigma_w)$  with positive semi-definite covariance  $\Sigma_w \in \mathbb{R}^{n_x \times n_x}$ , which leads to  $v(t) \sim \mathcal{N}(0, B_d^\dagger \Sigma_w B_d)$  in Eq. (3) – a common setup for GP-MPC as done, e.g., by [3].

A major challenge for GP-MPC is the propagation of state uncertainty, induced by the stochastic GP model of the unknown function  $g^{\text{tr}}$ . Commonly, a linearization-based approximation of the stochastic dynamics in terms of its mean  $\mu_k^x$  and covariance  $\Sigma_k$  is employed, which leads to the following approximate reformulation of the GP-MPC optimization problem [3],

$$\min_{\substack{u_0, \dots, u_{N-1} \\ \mu_0^x, \dots, \mu_N^x \\ \Sigma_0^x, \dots, \Sigma_N^x}} \sum_{k=0}^{N-1} l(\mu_k^x, u_k) + M(\mu_N^x) \quad (13a)$$

$$\text{s.t.} \quad \mu_0^x = \bar{x}_0, \quad (13b)$$

$$\Sigma_0^x = 0, \quad (13c)$$

$$\mu_{k+1}^x = f(\mu_k^x, u_k) + B_d g(\mu_k^x, u_k), \quad (13d)$$

$$\Sigma_{k+1}^x = \Psi_k(\mu_k^x, u_k, \Sigma_k^x), \quad (13e)$$

$$0 \geq h(\mu_k^x, u_k) + \beta(\mu_k^x, u_k, \Sigma_k^x), \quad (13f)$$

$$0 \geq h_N(\mu_N^x) + \beta_N(\mu_N^x, \Sigma_N^x). \quad (13g)$$

Thereby, the discrete-time covariance dynamics are given as

$$\Psi_k(\mu_k^x, u_k, \Sigma_k^x) = A_k \Sigma_k^x A_k^\top + B_d \Sigma^g(\mu_k^x, u_k) B_d^\top + \Sigma_w, \quad (14)$$

where  $A(\mu_k^x, u_k) \doteq \left. \frac{\partial}{\partial x} (f(x, u_k) + B_d g(x, u_k)) \right|_{x=\mu_k^x}$  denotes the Jacobian of the nominal and GP mean dynamics with respect to the (mean) state. Component-wise for each  $j = 1, \dots, n_h$ , the nominal constraints  $h_j$  are tightened by

$$\beta_j(\mu_k^x, u_k, \Sigma_k) \doteq \gamma_j \sqrt{C_j(\mu_k^x, u_k) \Sigma_k C_j^\top(\mu_k^x, u_k)}, \quad (15)$$

where  $C_j(\mu_k^x, u_k) = \left. \frac{\partial h_j}{\partial x} (x, u_k) \right|_{x=\mu_k^x}$ . Assuming a Gaussian state density,  $p_j = \Phi(\gamma_j)$  thereby corresponds to the approximate satisfaction probability of the linearized one-sided constraint, with  $\Phi(\cdot)$  denoting the cumulative density function of a standard normal Gaussian variable.

### B. Zero-order GP-MPC algorithm

Despite the approximations, the solution of the GP-MPC OCP (13) still remains intractable for many real-time applications: Propagation of the state covariances (13e) inside the optimal control problem (OCP) introduces a large additional number of optimization variables, which leads to an unfavorable scaling of the computational complexity with respect to the state dimension; additionally, expensive GP computations are to be performed, in particular for the gradients of the posterior covariance and for the Hessian of the posterior mean. To tackle these challenges, it has been proposed in [34] to employ the zero-order robust optimization (zoRO) method [30], [31], which performs sequential quadratic programming (SQP) with a tailored Jacobian approximation to obtain a suboptimal, yet feasible, point of the OCP (13) at drastically reduced computational cost. Starting with an initial guess for the input and mean variables  $\hat{u}_k$  and  $\hat{\mu}_k^x$ , respectively,

the zoRO algorithm propagates the covariances (13e) based on the previous SQP iterate  $(\hat{u}_k, \hat{\mu}_k^x)$ ,

$$\hat{\Sigma}_{k+1}^x = \Psi_k(\hat{\mu}_k^x, \hat{u}_k, \hat{\Sigma}_k^x), \quad k = 0, \dots, N-1, \quad (16)$$

before obtaining the next iterate by performing SQP iterations towards a Karush-Kuhn-Tucker (KKT) point of the reduced-size OCP

$$\min_{\substack{u_0, \dots, u_{N-1} \\ \mu_0^x, \dots, \mu_N^x}} \sum_{k=0}^{N-1} l(\mu_k^x, u_k) + M(\mu_N^x) \quad (17a)$$

$$\text{s.t.} \quad \mu_0^x = x(t), \quad (17b)$$

$$\mu_{k+1}^x = f(\mu_k^x, u_k) + B_d g(\mu_k^x, u_k), \quad (17c)$$

$$0 \geq h(\mu_k^x, u_k) + \hat{\beta}_k, \quad (17d)$$

$$0 \geq h_N(\mu_N^x) + \hat{\beta}_N. \quad (17e)$$

At each SQP iteration of the zoRO algorithm, the constraint tightenings in Eqs. (13f) and (13g), respectively, are thus fixed – hence, their Jacobians neglected – based on the iterates  $(\hat{\mu}_k^x, \hat{u}_k, \hat{\Sigma}_k^x)$  at the previous zoRO iteration, i.e.,

$$\hat{\beta}_k \doteq \beta(\hat{\mu}_k^x, \hat{u}_k, \hat{\Sigma}_k^x). \quad (18)$$

Due to the neglected Jacobian, the zoRO algorithm obtains a suboptimal, yet feasible, point of the OCP at convergence. Note that the presented version of the zoRO algorithm employs an additional Jacobian approximation compared to the one in [31], [34] by neglecting the entire Jacobians of the constraint tightenings, as it has also been done in [32], [37].

### C. Zero-order GP-MPC implementation using L4acados

Using L4acados, the zero-order GP-MPC method [34] is implemented by defining a GPyTorch [38] residual model for efficient and parallelizable GP computations, as well as extending the zoRO custom update function [37] in acados for efficient uncertainty propagation with BLASFEO [49].

1) *GPyTorch ResidualModel*: While the main function of the ResidualModel is to provide evaluations and sensitivities of the GP posterior mean, for the zoGPMPC implementation it has been extended to i) compute and store the GP posterior covariance; ii) perform input feature selection; iii) support various data processing strategies, facilitating the recording of data points as well as online GP model updates.

2) *acados custom update function*: In between SQP iterations, the zoGPMPC algorithm propagates the state covariances according to (14). To this end, the efficient zoRO implementation presented in [37], which utilizes the high-performance linear algebra package BLASFEO [49], has been extended to support a time-varying process noise component, which is used to incorporate evaluations of the GP posterior covariance in the covariance prediction.

### D. Autonomous miniature racing

The proposed implementation is tested on the CRS robotics software platform [39], which is used for autonomous racing in simulation<sup>3</sup> as well as on hardware<sup>4</sup>, using a custom 1:24

<sup>3</sup>Code: <https://gitlab.ethz.ch/ics/crs>

<sup>4</sup>Experiment data and video material: doi:10.3929/ethz-b-000707631.

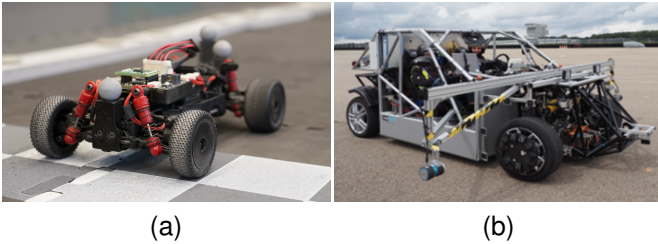


Fig. 4. Hardware platforms. Using L4acados, the zoGPMPC method is deployed on (a) a 1:24 miniature race car and (b) a full-scale test vehicle.

miniature R/C car based on a Mini-Z MB010 four-wheel drive chassis (see Fig. 4a) and a Qualisys motion capture system.

The controller is formulated akin to the model predictive contouring control (MPCC) formulation of [50, Eq. (13)], where the state  $\mu_k^x = (x, y, \psi, v_x, v_y, \omega, T, \delta, \theta) \in \mathbb{R}^9$  contains the mean  $x$ -,  $y$ -position and heading angle  $\psi$  in a global coordinate frame, lateral and longitudinal velocities  $v_x$  and  $v_y$ , as well as yaw rate  $\omega$  in a local coordinate frame, respectively. Additionally, the states  $T$  and  $\delta$  denote the applied torque and steering angle, respectively, and  $\theta$ , the progress of the car along the track. The nominal model is then composed of the combined dynamics of the kinematic bicycle model using a simplified Pacejka tire model (see, e.g., [39, Sec. V.A.2]), and simple integrators for the torque and steering angle's actuator dynamics, as well as for the progress variable. For the latter, the corresponding velocities are the control inputs  $u_k \doteq (\dot{T}, \dot{\delta}, \dot{\theta}) \in \mathbb{R}^3$ . The MPCC problem can then be expressed as problem (13) with zero terminal cost,  $M(\mu_N^x) = 0$ , and a nonlinear-least-squares stage cost  $l(\mu_k^x, u_k) = \|y(\mu_k^x, u_k)\|_{Q^y}^2$ , where the regressor  $y(\mu_k^x, u_k) = (e^c(x_k, y_k, \theta_k), e^l(x_k, y_k, \theta_k), \dot{T}_k, \dot{\delta}_k, \dot{\theta}_k, 1)$  contains the contouring and lag error terms  $e^c$  and  $e^l$ , respectively, as well as the inputs  $\dot{T}_k, \dot{\delta}_k, \dot{\theta}_k$ . Using the additional constant term, the MPCC cost can be expressed by appropriately defining the positive definite penalty matrix  $Q^y$ .

As the most severe modeling errors are considered to be in the Pacejka tire friction model and corresponding parameter estimates, a GP is used to learn the residual of the discrete-time velocity predictions, i.e.,  $B_d^\top \doteq [0_{3 \times 3} \quad I_{3 \times 3} \quad 0_{3 \times 3}]$ . To reduce the dimensionality of the input space, and the associated risk of overfitting to irrelevant features, the GP input features are chosen as  $(v_x, v_y, \omega, T, \delta)$ .

1) *Simulation results:* To evaluate computation times in a more controlled environment for different solver configurations, runtime experiments are performed in a ROS simulation for a fixed number of  $N_{\text{sim}} = 3000$  simulation steps at a sampling frequency of 30Hz, amounting to a 100s time limit. The ground-truth car dynamics is thereby simulated using a set of Pacejka friction parameters obtained from system identification on the real system, while the nominal car dynamics use values that have been slightly perturbed; in particular, the perturbed model assumes rear-wheel drive instead of four-wheel drive and over-estimates the grip, leading to unsafe driving behavior.

Fig. 5 shows the closed-loop constraint evaluation of the

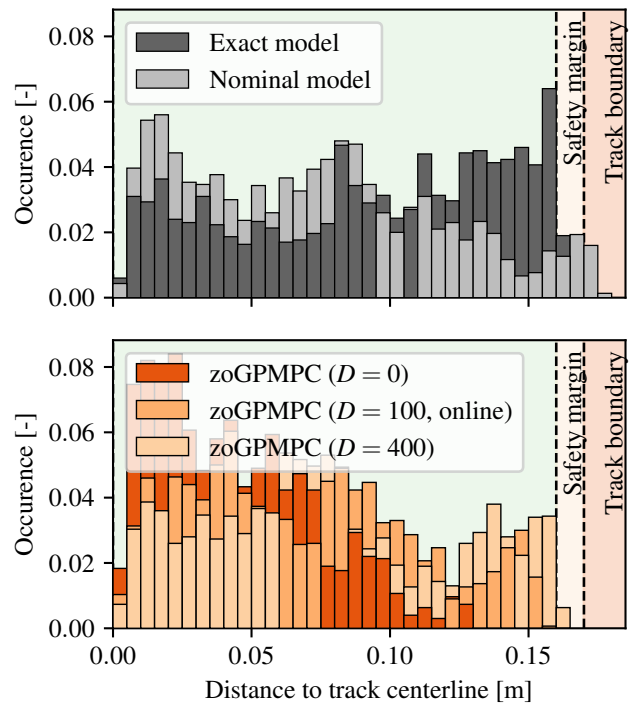


Fig. 5. Distance between miniature race car and centerline in closed-loop simulations. Augmented with real-world data, the uncertainty-aware GP model reduces conservatism to cautiously improve driving performance.

track constraint for SQP-RTI controllers using different models. Separated by the dashed lines, the green zone denotes the (soft) constraint implemented in the controller; the yellow zone, an additional safety margin to the track boundary; the red zone, the track limits. In the top plot, it can be seen that the controller based on the exact model operates close to the track constraint. While for the exact model the car stays within the defined safety margins at all times, for the nominal model track constraint violations (i.e. crashes) occur. The small proportion of (soft) constraint violations using the exact model can be attributed to approximate convergence within the real-time iterations, as well as delays in the ROS simulator. In the lower plot, the constraint evaluations for the zoGPMPC method are shown. For  $D = 0$  data points, i.e., the prior GP uncertainty, the car stays close to the centerline; for  $D \in \{100, 400\}$  points, much more aggressive driving behavior is observed. Notably, in all cases, the track constraints are respected, showcasing the potential for high-performance, yet uncertainty-aware, learning-based control.

In Table I, a variety of solver configurations is compared:

*Covariance:* *zero-order* covariances denote recomputed constraint tightenings at each SQP iteration, in contrast to *fixed* covariances based on the predicted trajectory at the previous sampling time<sup>6</sup>; both variants are equivalent for *SQP-RTI*.

*Optimizer:* *SQP* is used to solve the OCP iteratively at each sampling time until convergence while *SQP-RTI* performs a single iteration at each sampling time. For the simulations, an iterate with all KKT residuals smaller than  $\text{tol} \doteq 10^{-4}$  is considered converged; the maximum number of SQP iterations is set to 30. To meet sampling time requirements for all

TABLE I  
PERFORMANCE COMPARISON OF DIFFERENT GP-MPC VARIANTS IN SIMULATION FOR AUTONOMOUS MINIATURE RACING.

| Name                        | Covariance | Optimizer | GP Model     | $D$ | Time, total <sup>5</sup> | Time, prep <sup>5</sup> | Time, fdbk <sup>5</sup> | Cost <sup>5</sup> | Laps <sup>5</sup> | Crashed |
|-----------------------------|------------|-----------|--------------|-----|--------------------------|-------------------------|-------------------------|-------------------|-------------------|---------|
| Exact model                 | -          | SQP-RTI   | -            | -   | 5.9 ± 1.1                | 3.3 ± 0.6               | 2.6 ± 0.6               | 3.4               | 20.3              |         |
| Nominal model               | -          | SQP-RTI   | -            | -   | 6.0 ± 0.6                | 3.3 ± 0.3               | 2.6 ± 0.3               | 3.5               | 20.4              | ✗       |
| zoGPMPC                     | zero-order | SQP-RTI   | exact        | 0   | 6.6 ± 0.5                | 4.2 ± 0.3               | 2.4 ± 0.3               | 4.3               | 15.7              |         |
| zoGPMPC                     | zero-order | SQP-RTI   | exact        | 400 | 11.9 ± 0.9               | 9.5 ± 0.7               | 2.4 ± 0.3               | 3.6               | 19.4              |         |
| zoGPMPC                     | zero-order | SQP-RTI   | inducing     | 400 | 35.5 ± 1.7               | 33.1 ± 1.6              | 2.4 ± 0.3               | 3.6               | 19.4              |         |
| zoGPMPC                     | zero-order | SQP-RTI   | exact/online | 100 | 16.5 ± 2.0               | 14.1 ± 1.9              | 2.5 ± 0.3               | 3.9               | 17.2              |         |
| Exact model                 | -          | SQP       | -            | -   | 91.7 ± 36.5              | 2.6 ± 0.3               | 89.0 ± 36.5             | 3.4               | 20.8              |         |
| Nominal model               | -          | SQP       | -            | -   | 96.8 ± 40.1              | 2.6 ± 0.2               | 94.2 ± 40.1             | 3.5               | 21.1              | ✗       |
| zoGPMPC                     | zero-order | SQP       | exact        | 0   | 121.2 ± 38.6             | 3.5 ± 0.3               | 117.7 ± 38.5            | 4.2               | 16.4              |         |
| zoGPMPC                     | zero-order | SQP       | exact        | 400 | 238.9 ± 92.9             | 8.6 ± 0.5               | 230.3 ± 92.9            | 3.5               | 20.1              |         |
| Cautious GPMPC <sup>6</sup> | fixed      | SQP       | exact        | 400 | 173.8 ± 67.8             | 8.5 ± 0.9               | 165.3 ± 67.7            | 3.5               | 20.2              |         |

methods, the simulation time is scaled by  $\alpha_{RTI} \doteq 0.5$  for *SQP-RTI* scenarios and by  $\alpha_{SQP} \doteq 0.015$  for *SQP* scenarios.

*GP model:* All GP models are implemented using `GPYTORCH` [38]. The *exact* GP model obtains the posterior mean and covariance using an (offline) Cholesky decomposition of the kernel matrix; the *inducing*-point GP model, using the subset-of-regressors approximation [51, Sec. 8.3.1] with 10 inducing points, re-distributed along the previously predicted input-feature trajectories at each sampling time; the *online* implementation, an exact GP model incorporating new data points at every sampling time, randomly replacing old data points once a pre-specified limit is reached, with recursive up- and down-dates of the kernel matrix’ Cholesky factors (see, e.g., [52, Appendix B]).

*Time:* Total computation times (*total*) are split into preparation (*prep.*) and feedback (*fdbk.*), the former including all computations that can be performed before sampling the next initial state, the latter, the remaining computations.

*Cost:* This column shows the average stage cost for the closed-loop trajectory i.e.,  $\frac{1}{N_{sim}} \sum_{t=1}^{N_{sim}} l(x(t), u(t))$ .

*Laps:* The progress made within the  $N_{sim}$  simulation steps, in terms of the number of laps completed, is shown here.

*Crash:* To compensate for delays, approximate convergence and unmodeled real-world effects, the (soft) track constraint is tightened by an additional safety margin (see Fig. 5). An “✗” indicates violation of the original track constraint.

Comparing the optimizer, it can be seen that throughout all experiments, *SQP* performs slightly better than its *SQP-RTI* counterpart in terms of closed-loop cost and track progress, at the expense of considerably increased computation times due to the higher number of *SQP* iterations. Regarding the GP model, the inducing-point approximation performs similarly well as the exact GP model; however, perhaps surprisingly, at a higher computational cost. This may be attributed to the fact that the exact GP model allows one to reuse the precomputed Cholesky factor, while re-distributing inducing points at each sampling time requires one to refactorize the approximated covariance matrix. The online-updating version of the exact

model is real-time feasible up to roughly 100 data points.

2) *Hardware experiments:* The racing experiment has been repeated on hardware (see Fig. 1) using the three *SQP-RTI* variants of zoGPMPC in Table I with an exact GP model; Fig. 6 shows the corresponding closed-loop trajectories and car velocities. As expected, the “unconditioned” variant with  $D = 0$  data points in Fig. 6a) keeps the car closer to the centerline<sup>7</sup>. Fig. 6b) shows the zoGPMPC method with  $D = 400$  random data points recorded in the previous “unconditioned” experiment: The car drives significantly more aggressively, at higher speeds and taking sharper corners. A similar driving performance is achieved using the online learning strategy with  $D = 100$  data points; the transition from a more cautious to a more aggressive racing line is apparent in Fig. 6c) and d), which depict the first and sixth lap of the same experiment, respectively.

### E. Motion control of full-scale vehicle

To demonstrate its applicability, `L4ACADOS` is used for safe learning-based control of a research vehicle (Fig. 4b). The controller is formulated similarly to the autonomous-racing case in Section IV-D, using a slightly modified system model with states  $\mu_k^x = (x, y, \psi, v, \beta, \omega, \delta, \delta_{des}, a_x, \theta) \in \mathbb{R}^{10}$  and inputs  $u_k \doteq (\dot{a}_x, \dot{\delta}, \dot{\theta}) \in \mathbb{R}^3$ . Here, the slip angle  $\beta$  and the effective velocity  $v$  are a different representation of  $v_x, v_y$  in Section IV-D. The additional states  $\delta_{des}$  and  $\delta$  represent a first-order lag element to capture the steer-by-wire dynamics;  $a_x$ , the desired acceleration interface provided by the vehicle platform. The model is discretized for  $N = 20$  steps using 4th-order Runge-Kutta integrator with step size 0.1 [s]. The motion control task is to comfortably track a given path with a reference velocity  $v_{ref}$ , yielding the modified regressor  $y(\mu_k^x, u_k) = (e_k^c, e_k^l, v_k, \omega_k, \dot{a}_k, \delta_{des,k}, \dot{\theta}_k, v_{ref})$ ,

<sup>5</sup>Entries are rounded to the first significant digit. “ $a \pm b$ ” indicates “mean computation time  $a$  with standard deviation  $b$ ”, in milliseconds.

<sup>6</sup>While not exactly corresponding to the original implementation, which employed a commercial interior-point solver, this variant uses fixed covariances based on the last sampling time during optimization while solving the OCP (with correspondingly fixed tightenings) to convergence, as done in [3].

<sup>7</sup>Noteworthy, due to the neglected Jacobians of the covariances with respect to the states and inputs in the optimizer, the *zero-order* method, and the *fixed* variant, do not take the effect of the inputs on the size of the covariances; the reduction of the car velocity follows solely from the tighter track constraint, forcing the car to stay on the centerline.

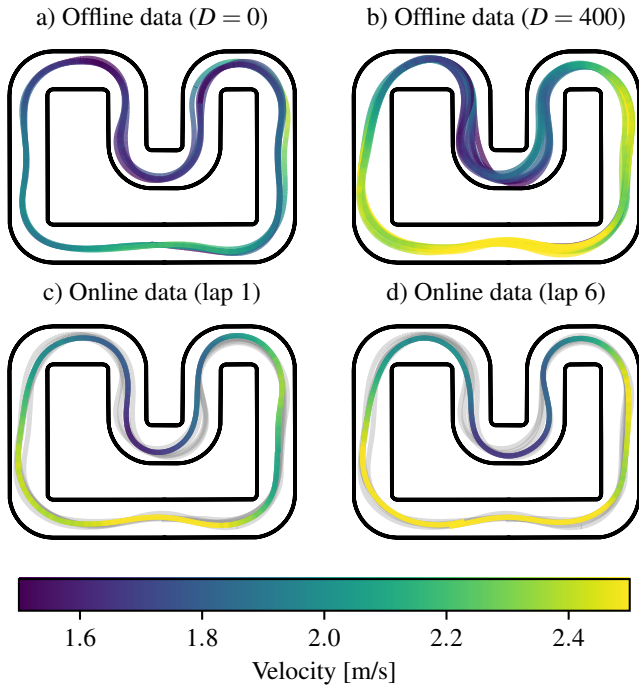


Fig. 6. Closed-loop performance comparison in miniature-racing hardware experiments (Section IV-D). In the offline and online learning setting, augmenting the nominal model with a GP leads to improved driving performance.

subject to the safety-critical constraint of staying within the track boundaries and box constraints  $\beta \in [-0.17, 0.17]$  [rad],  $v \in [0.5, 40]$  [m/s],  $\delta, \delta_{\text{des}} \in [0.61, 0.61]$  [rad],  $\dot{\delta}_{\text{des}} \in [-0.35, 0.35]$  [rad/s],  $a_x \in [-5, 5]$  [m/s<sup>2</sup>],  $\dot{a}_x \in [-4, 4]$  [m/s<sup>3</sup>]. The GP is used to correct velocity predictions and the steering dynamics, i.e.,  $B_d \doteq [0_{3 \times 4} \quad I_{4 \times 4} \quad 0_{3 \times 4}]$ , with GP inputs  $(v, \beta, \omega, \delta, \delta_{\text{des}}, a_x)$ .

We show the effect of including the GP model via `L4acados` using a double lane change maneuver based on the ISO 3888-1 standard (without an increasing corridor) at 30 km/h, see Fig. 7. First, a basic nominal model parameterization is applied, with *SQP-RTI*. The control performance is unsatisfactory in terms of actuator load, comfort, and stable tracking of the desired path. Equally spaced data points along the driven path are used to fit an exact GP model as described in Section IV-D using basic data preprocessing. The experiment was repeated with the same nominal model extended by the GP correction term, with a desired probability level of  $p_x \doteq 95\%$  for satisfying the safety-critical path constraint. The result shows significant improvements in all performance aspects: Reduced actuation requests lead to a more comfortable driving experience, and accurate tracking of the desired path provides stable behavior. Furthermore, while the predicted confidence estimate is mostly contained within the path constraints, larger uncertainties at the end of the planning horizon act similar to a small terminal set constraint, further stabilizing the performance. The computations performed on an HP Zbook 16 Fury G10 notebook resulted in total computation times as shown in Table II – well within the control cycle time of 20ms.

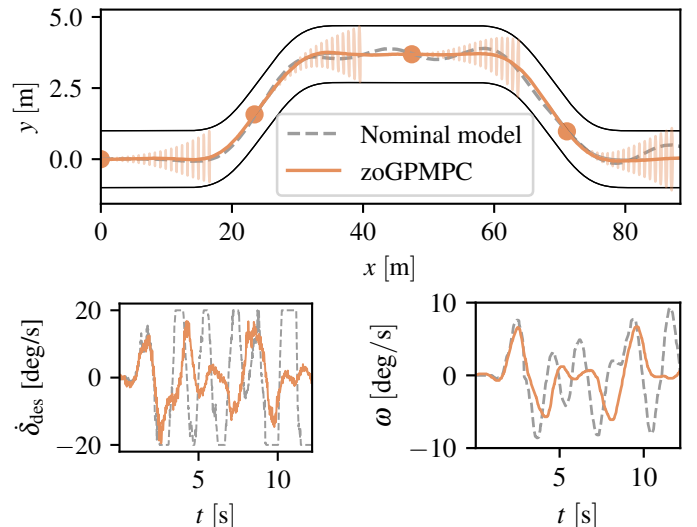


Fig. 7. Double lane change maneuver of the full-scale vehicle (Figure 4b) at 30 km/h. The nominal MPC controller yields unsatisfactory performance; the zoGPMPC method provides significant improvements. The bars indicate 95% confidence intervals that are used to tighten the track boundary constraints.

TABLE II  
TOTAL COMPUTATION TIMES FOR FULL-SCALE EXPERIMENT.

| Name       | Covariance | Optimizer | GP    | $D$ | Time, total <sup>5</sup> |
|------------|------------|-----------|-------|-----|--------------------------|
| Nominal m. | -          | SQP-RTI   | -     | -   | $3.1 \pm 1.4$            |
| zoGPMPC    | zero-order | SQP-RTI   | exact | 136 | $8.2 \pm 1.4$            |

## V. CONCLUSIONS AND OUTLOOK

In this paper, we presented a method for incorporating external (learning-based) sensitivity information into optimal control solvers. For the common use case of learning-based Python models in the optimal control software `acados`, we provide `L4acados`; the efficiency and applicability of the software is demonstrated i) in a benchmark against available software for a neural network-based MPC example and ii) by simulation and hardware experiments using Gaussian process-based MPC for autonomous miniature racing and a full-scale autonomous vehicle prototype. For future work, extensions to learning-based constraint and cost modules, as well as full integration of external, batched sensitivity computations in `acados`, can further increase its range of potential applications and ease of use.

## ACKNOWLEDGMENT

The authors would like to thank Tim Salzmann for a clarifying discussion regarding the benefits and limitations of `L4acados` compared to `L4CasADi`, as well as Lars Bartels and Alexander Hansson for their contributions to `L4acados`.

## REFERENCES

- [1] L. Hewing, K. P. Wabersich, M. Menner, and M. N. Zeilinger, "Learning-Based Model Predictive Control: Toward Safe Learning in Control," *Annual Review of Control, Robotics, and Autonomous Systems*, vol. 3, no. 1, 2020.

- [2] J. Kabzan, L. Hewing, A. Liniger, and M. N. Zeilinger, "Learning-Based Model Predictive Control for Autonomous Racing," *IEEE Robotics and Automation Letters*, vol. 4, no. 4, 2019.
- [3] L. Hewing, J. Kabzan, and M. N. Zeilinger, "Cautious Model Predictive Control Using Gaussian Process Regression," *IEEE Transactions on Control Systems Technology*, vol. 28, no. 6, 2020.
- [4] N. A. Spielberg, M. Brown, and J. C. Gerdes, "Neural Network Model Predictive Motion Control Applied to Automated Driving With Unknown Friction," *IEEE Transactions on Control Systems Technology*, vol. 30, no. 5, 2022.
- [5] G. Torrente, E. Kaufmann, P. Föhn, and D. Scaramuzza, "Data-Driven MPC for Quadrotors," *IEEE Robotics and Automation Letters*, vol. 6, no. 2, 2021.
- [6] K. Y. Chee, T. Z. Jiahao, and M. A. Hsieh, "KNODE-MPC: A Knowledge-Based Data-Driven Predictive Control Framework for Aerial Robots," *IEEE Robotics and Automation Letters*, vol. 7, no. 2, 2022.
- [7] A. Saviolo, G. Li, and G. Loianno, "Physics-Inspired Temporal Learning of Quadrotor Dynamics for Accurate Model Predictive Trajectory Tracking," *IEEE Robotics and Automation Letters*, vol. 7, no. 4, 2022.
- [8] J. Li, L. Han, H. Yu, Y. Lin, Q. Li, and Z. Ren, "Nonlinear MPC for Quadrotors in Close-Proximity Flight with Neural Network Downwash Prediction," in *2023 62nd IEEE Conference on Decision and Control (CDC)*, 2023.
- [9] K. Y. Chee, P.-A. Hsieh, G. J. Pappas, and M. A. Hsieh, "Flying Quadrotors in Tight Formations using Learning-based Model Predictive Control," 2024.
- [10] C. J. Ostafew, A. P. Schoellig, and T. D. Barfoot, "Learning-based nonlinear model predictive control to improve vision-based mobile robot path-tracking in challenging outdoor environments," in *2014 IEEE International Conference on Robotics and Automation (ICRA)*, 2014.
- [11] —, "Robust Constrained Learning-based NMPC enabling reliable mobile robot path tracking," *The International Journal of Robotics Research*, vol. 35, no. 13, 2016.
- [12] A. Carron, E. Arcari, M. Wermelinger, L. Hewing, M. Hutter, and M. N. Zeilinger, "Data-Driven Model Predictive Control for Trajectory Tracking With a Robotic Arm," *IEEE Robotics and Automation Letters*, vol. 4, no. 4, 2019.
- [13] J. Bradbury, R. Frostig, P. Hawkins, M. J. Johnson, C. Leary, D. Maclaurin, G. Necula, A. Paszke, J. VanderPlas, S. Wanderman-Milne, and Q. Zhang, "JAX: Composable transformations of Python+NumPy programs," 2018. [Online]. Available: <http://github.com/google/jax>
- [14] A. Paszke, S. Gross, F. Massa, A. Lerer, J. Bradbury, G. Chanan, T. Killeen, Z. Lin, N. Gimelshein, L. Antiga, A. Desmaison, A. Kopf, E. Yang, Z. DeVito, M. Raison, A. Tejani, S. Chilamkurthy, B. Steiner, L. Fang, J. Bai, and S. Chintala, "PyTorch: An Imperative Style, High-Performance Deep Learning Library," in *Advances in Neural Information Processing Systems 32*. Curran Associates, Inc., 2019.
- [15] T. Developers, "TensorFlow," 2025. [Online]. Available: <https://zenodo.org/doi/10.5281/zenodo.4724125>
- [16] J. A. E. Andersson, J. Gillis, G. Horn, J. B. Rawlings, and M. Diehl, "CasADI: A software framework for nonlinear optimization and optimal control," *Mathematical Programming Computation*, vol. 11, no. 1, 2019.
- [17] R. Verschueren, G. Frison, D. Kouzoupis, J. Frey, N. van Duijkeren, A. Zanelli, B. Novoselnik, T. Albin, R. Quirynen, and M. Diehl, "Acados—a modular open-source framework for fast embedded optimal control," *Mathematical Programming Computation*, vol. 14, no. 1, 2022.
- [18] Z. Yuan, A. W. Hall, S. Zhou, L. Brunke, M. Greeff, J. Panerati, and A. P. Schoellig, "Safe-Control-Gym: A Unified Benchmark Suite for Safe Learning-Based Control and Reinforcement Learning in Robotics," *IEEE Robotics and Automation Letters*, vol. 7, no. 4, 2022.
- [19] D. C. Gordon, A. Winkler, J. Bedei, P. Schaber, S. Pischinger, J. Andert, and C. R. Koch, "Introducing a Deep Neural Network-Based Model Predictive Control Framework for Rapid Controller Implementation," in *2024 American Control Conference (ACC)*, 2024.
- [20] T. Z. Jiahao, K. Y. Chee, and M. A. Hsieh, "Online Dynamics Learning for Predictive Control with an Application to Aerial Robots," in *Proceedings of The 6th Conference on Robot Learning*. PMLR, 2023.
- [21] R. Jia, X. Zhao, S. Zhang, and X. Yu, "A Tube-NMPC Approach for Robust Control of Glucose in Type 1 Diabetes Mellitus," *IEEE Transactions on Automation Science and Engineering*, 2024.
- [22] T. Salzmann, E. Kaufmann, J. Arrizabalaga, M. Pavone, D. Scaramuzza, and M. Ryll, "Real-Time Neural MPC: Deep Learning Model Predictive Control for Quadrotors and Agile Robotic Platforms," *IEEE Robotics and Automation Letters*, vol. 8, no. 4, 2023.
- [23] F. Fiedler, B. Karg, L. Lüken, D. Brandner, M. Heinlein, F. Brabender, and S. Lucia, "Do-mpc: Towards FAIR nonlinear and robust model predictive control," *Control Engineering Practice*, vol. 140, 2023.
- [24] T. L. Foundation, "ONNX." [Online]. Available: <https://onnx.ai/>
- [25] J. Pohlodek, B. Morabito, C. Schlauch, P. Zometa, and R. Findeisen, "Flexible development and evaluation of machine-learning-supported optimal control and estimation methods via HILO-MPC," *International Journal of Robust and Nonlinear Control*, vol. n/a, no. n/a, 2024.
- [26] E. Picotti, A. D. Libera, R. Carli, and M. Bruschetta, "LbMATMPC: An open-source toolbox for Gaussian Process modeling within Learning-based Nonlinear Model Predictive Control," in *2022 European Control Conference (ECC)*, 2022.
- [27] T. Salzmann, J. Arrizabalaga, J. Andersson, M. Pavone, and M. Ryll, "Learning for CasADI: Data-driven Models in Numerical Optimization," in *Proceedings of the 6th Annual Learning for Dynamics & Control Conference*. PMLR, 2024.
- [28] F. Panetsos, G. C. Karras, and K. J. Kyriakopoulos, "GP-based NMPC for Aerial Transportation of Suspended Loads," *IEEE Robotics and Automation Letters*, 2024.
- [29] B. Zarrouki, J. Nunes, and J. Betz, "R<sup>2</sup>NMPC: A Real-Time Reduced Robustified Nonlinear Model Predictive Control with Ellipsoidal Uncertainty Sets for Autonomous Vehicle Motion Control," *IFAC-PapersOnLine*, vol. 58, no. 18, 2024.
- [30] X. Feng, S. D. Cairano, and R. Quirynen, "Inexact Adjoint-based SQP Algorithm for Real-Time Stochastic Nonlinear MPC," *IFAC-PapersOnLine*, vol. 53, no. 2, 2020.
- [31] A. Zanelli, J. Frey, F. Messerer, and M. Diehl, "Zero-Order Robust Nonlinear Model Predictive Control with Ellipsoidal Uncertainty Sets," *IFAC-PapersOnLine*, vol. 54, no. 6, 2021.
- [32] Y. Gao, F. Messerer, J. Frey, N. van Duijkeren, and M. Diehl, "Collision-free Motion Planning for Mobile Robots by Zero-order Robust Optimization-based MPC," in *2023 European Control Conference (ECC)*, 2023.
- [33] S. Vaskov, R. Quirynen, M. Menner, and K. Berntorp, "Friction-Adaptive Stochastic Predictive Control for Trajectory Tracking of Autonomous Vehicles," in *2022 American Control Conference (ACC)*, 2022.
- [34] A. Lahr, A. Zanelli, A. Carron, and M. N. Zeilinger, "Zero-order optimization for Gaussian process-based model predictive control," *European Journal of Control*, vol. 74, 2023.
- [35] P. Polcz, T. Péni, and R. Tóth, "Efficient implementation of Gaussian process-based predictive control by quadratic programming," *IET Control Theory & Applications*, vol. 17, no. 8, 2023.
- [36] M. Diehl, H. G. Bock, and J. P. Schlöder, "A Real-Time Iteration Scheme for Nonlinear Optimization in Optimal Feedback Control," *SIAM Journal on Control and Optimization*, vol. 43, no. 5, 2005.
- [37] J. Frey, Y. Gao, F. Messerer, A. Lahr, M. N. Zeilinger, and M. Diehl, "Efficient Zero-Order Robust Optimization for Real-Time Model Predictive Control with acados," 2023.
- [38] J. Gardner, G. Pleiss, K. Q. Weinberger, D. Bindel, and A. G. Wilson, "GPY Torch: Blackbox Matrix-Matrix Gaussian Process Inference with GPU Acceleration," in *Advances in Neural Information Processing Systems*, vol. 31. Curran Associates, Inc., 2018.
- [39] A. Carron, S. Bodmer, L. Vogel, R. Zurbrügg, D. Helm, R. Rickenbach, S. Muntwiler, J. Sieber, and M. N. Zeilinger, "Chronos and CRS: Design of a miniature car-like robot and a software framework for single and multi-agent robotics and control," in *2023 IEEE International Conference on Robotics and Automation (ICRA)*, 2023.
- [40] G. Torrisi, D. Frick, T. Robbiani, S. Grammatico, R. S. Smith, and M. Morari, "FalcOpt: First-order algorithm via linearization of constraints for optimization," 2017. [Online]. Available: <https://github.com/torrisig/FalcOpt>
- [41] M. Gifftthaler, M. Neunert, M. Stäuble, and J. Buchli, "The control toolbox — An open-source C++ library for robotics, optimal and model predictive control," in *2018 IEEE International Conference on Simulation, Modeling, and Programming for Autonomous Robots (SIMPAP)*, 2018.
- [42] P. Listov and C. Jones, "PolyMPC: An efficient and extensible tool for real-time nonlinear model predictive tracking and path following for fast mechatronic systems," *Optimal Control Applications and Methods*, vol. 41, no. 2, 2020.
- [43] Y. Chen, M. Bruschetta, E. Picotti, and A. Beghi, "MATMPC - A MATLAB Based Toolbox for Real-time Nonlinear Model Predictive Control," in *2019 18th European Control Conference (ECC)*, 2019.
- [44] T. Englert, A. Völz, F. Mesmer, S. Rhein, and K. Graichen, "A software framework for embedded nonlinear model predictive control using a gradient-based augmented Lagrangian approach (GRAMPC)," *Optimization and Engineering*, vol. 20, no. 3, 2019.

- [45] P. T. Boggs and J. W. Tolle, "Sequential quadratic programming," *Acta Numerica*, vol. 4, 1995.
- [46] J. Frey, J. D. Schutter, and M. Diehl, "Fast integrators with sensitivity propagation for use in CasADi," in *2023 European Control Conference (ECC)*, 2023.
- [47] H. G. Bock, M. Diehl, E. Kostina, and J. P. Schlöder, "1. Constrained Optimal Feedback Control of Systems Governed by Large Differential Algebraic Equations," in *Real-Time PDE-Constrained Optimization*. Society for Industrial and Applied Mathematics, 2007.
- [48] L. Numerow, A. Zanelli, A. Carron, and M. N. Zeilinger, "Inherently Robust Suboptimal MPC for Autonomous Racing With Anytime Feasible SQP," *IEEE Robotics and Automation Letters*, vol. 9, no. 7, 2024.
- [49] G. Frison, D. Kouzoupis, T. Sartor, A. Zanelli, and M. Diehl, "BLAS-FEO: Basic Linear Algebra Subroutines for Embedded Optimization," *ACM Transactions on Mathematical Software*, vol. 44, no. 4, 2018.
- [50] A. Liniger, A. Domahidi, and M. Morari, "Optimization-based autonomous racing of 1:43 scale RC cars," *Optimal Control Applications and Methods*, vol. 36, no. 5, 2015.
- [51] C. E. Rasmussen and C. K. I. Williams, *Gaussian Processes for Machine Learning*, ser. Adaptive Computation and Machine Learning. Cambridge, Massachusetts: MIT Press, 2006.
- [52] M. A. Osborne, "Bayesian Gaussian processes for sequential prediction, optimisation and quadrature," Ph.D. dissertation, Oxford University, UK / Oxford University, UK, 2010.